From quantum ladder climbing to classical autoresonance

G. Marcus, L. Friedland, and A. Zigler
Racah Institute of Physics, Hebrew University of Jerusalem, 91904 Jerusalem, Israel
(Received 12 August 2003; published 21 January 2004)

The autoresonance phenomenon allows excitation of a classical, oscillatory nonlinear system to high energies by using a weak, chirped frequency forcing. Ladder climbing is its counterpart in quantum mechanics. Here, for the first time to our knowledge, conditions for the transition from the quantum to the classical regimes are outlined. The similarities and differences between the two approaches are presented.

DOI: 10.1103/PhysRevA.69.013407 PACS number(s): 42.50.Hz, 33.80.Gj, 33.80.Wz

I. INTRODUCTION

The ability to place an atom or a molecule in a specific state is of great importance in spectroscopy and chemical dynamics [1]. Direct excitation of high vibrational levels in a molecule by monochromatic radiation is inefficient, due to the small value of the transition dipole moment between the initial and final states [2]. An alternative is to create a cascading transition from the initial to the final state through a series of intermediate levels by using a chirped light pulse having a continuously varying frequency. Several authors have addressed this problem, both classically and in quantum-mechanical terms [2–6]. In quantum mechanics the method is usually referred to as ladder climbing, while in classical mechanics the term dynamic autoresonance is used. Studying the problem of molecular excitation by a chirped pulse via classical mechanics yields a significant simplification and tractability of the details of the dynamics during the excitation [4,5]. However, the question of whether the classical approach is applicable in this case to quantum systems such as molecules is still open. In the present work we discuss the differences and similarities between the two approaches and study the transition from ladder climbing to dynamic autoresonance, where classical mechanics can be applied. We review the autoresonance and ladder climbing concepts in Secs. II and III. The two regimes are compared in Sec. IV, while numerical illustrations of our analysis are given in Sec. V. Finally, Sec. VI presents a summary of our results.

II. CLASSICAL DYNAMIC AUTORESONANCE

Dynamic autoresonance (AR) is a method of exciting an oscillatory nonlinear system to high energies by a weak driving oscillation, as well as controlling the excited state by changing the driving frequency. This method is general and has been applied in many fields of physics, such as particle accelerators [7], fluid dynamics [8], plasmas [9,10], nonlinear waves [11,12], and planetary dynamics [13,14]. For better understanding of the classical AR and, later, the ladder climbing (LC) phenomena, let us address the general problem of controllable excitation of a nonlinear oscillatory system from rest in classical terms. One can apply a resonant driving force for excitation, i.e., tune the drive frequency ω to the unperturbed system's natural response frequency ω_0. Nevertheless, in most cases, the nonlinear frequency shift destroys the resonance as the energy of oscillations increases, limiting the response amplitude to $O(\varepsilon^{1/2})$, where ε is the driving amplitude. In order to overcome this limitation one could start in resonance and later change the driving frequency, so that it continuously matches the instantaneous frequency of the driven system. Such a feedback approach allows one to stay in resonance for longer times, but frequency chirping by itself is not sufficient for ensuring continuing energy flow into the system. One also needs to correlate the phase of the drive to guarantee the stability of the time varying, phase-locked excited state. Furthermore, in microscopic systems such as atoms and molecules, it is usually difficult to both track and control the phase. Can we avoid using the feedback mechanism for strong excitation? The answer to this question is positive, and the idea is based on slow passage through the linear resonance in the system, instead of starting in resonance. One can show in this case that trapping into resonance followed by a continuing and stable self-phase-locking with the drive is guaranteed, provided the driving frequency chirp rate is small enough. This slow passage through and capture into resonance yields efficient control of the energy of the driven system, as it automatically (without external feedback) adjusts its state to stay in resonance with the chirped frequency drive. This is the essence of the dynamic autoresonance in the system.

For illustrating the AR in a simple case, consider a weakly nonlinear oscillator described by

$$u_{tt}+\omega_0^2 u+(cu^2+du^3)/m=0. \tag{1}$$

By decomposing the solution into harmonics $u\approx a_0+a_1\cos(\Omega t)+a_2\cos(2\Omega t)+\cdots$ and viewing the amplitude a_1 as small, one can calculate the natural response frequency of the oscillator to second order in a_1 [15]:

$$\Omega\approx\omega_0(1-\beta_c a_1^2), \tag{2}$$

where

$$\beta_c\approx\frac{3}{8}\left(\frac{c}{m\omega_0^2}\right)^2-\frac{5}{12}\frac{d}{m\omega_0^2}.$$

Now, consider a weakly driven oscillator

$$u_{tt}+\omega_0^2 u+(cu^2+du^3)/m=(\varepsilon/m)\cos\left[\int\omega(t)dt\right], \tag{3}$$

where $\omega=\omega_0(1-\alpha t)$, and both the chirp rate α and ε are small. To solve Eq. (3), we again expand u in harmonics: $u \approx a_0(t)+a_1(t)\cos[\theta(t)]+a_2(t)\cos[2\theta(t)]+\cdots$ but now view both $a_i(t)$ and the frequency of oscillations $\Omega(t)\equiv d\theta/dt$ as slow functions of time. Inserting this expansion into Eq. (3) and keeping resonant terms only yields the following slow evolution equations:

$$a_{1t}=-\frac{\varepsilon}{2m\omega_0}\sin\Phi, \tag{4a}$$

$$\Phi_t=\omega_0\beta_c a_1^2-\alpha t-\frac{\varepsilon}{2m\omega_0 a_1}\cos\Phi, \tag{4b}$$

where $\Phi(t)=\theta-\int\omega(t)dt$ is the phase mismatch and $[\ ]_t$ stand for $d[\ ]/dt$. At this stage, we introduce the dimensionless time $\tau=\alpha^{1/2}t$, the driving parameter $\mu=\frac{1}{2}(\varepsilon/m\omega_0)\times(\omega_0\beta_c)^{1/2}\alpha^{-3/4}$, and the rescaled complex dependent variable $\Psi=(\omega_0\beta_c)^{1/2}\alpha^{-1/4}a_1\exp(i\Phi)$. This allows us to convert our two real equations (4a) and (4b) into one complex equation for Ψ, with μ being a *single* parameter in the problem:

$$i\Psi_\tau+(|\Psi|^2-\tau)\Psi=\mu. \tag{5}$$

Equation (5) has two nonvanishing asymptotic solutions at $\tau\to+\infty$. One is the bounded solution $\Psi=a_1\exp(-i\tau^2/2)$, where the phase mismatch $\Phi\equiv\arg\Psi=-i\tau^2/2$ is growing continuously. The second solution is $\Psi=\tau^{1/2}$, where the amplitude $a_1=\tau^{1/2}$ is growing in time, but the phase mismatch remains zero. The transition between the bounded and unbounded solutions for a given initial condition $a_1=0$ at $\tau\to-\infty$ (the oscillator is at rest initially) is controlled by single parameter μ in Eq. (5). One finds numerically that the bifurcation occurs at $\mu_{th}\approx0.41$. Above this value, the phase locking persists and the amplitude grows continuously, while below μ_{th} the excitation dephases from the drive and saturates. By returning to the original parameters, we find the threshold forcing amplitude

$$\varepsilon_{th}=0.82m(\omega_0/\beta_c)^{1/2}\alpha^{3/4} \tag{6}$$

for having continuing phase locking (autoresonance) in the system. Alternatively, given the driving amplitude ε, one can achieve phase locking and growing amplitude excitation, provided the driving frequency chirp rate is sufficiently small,

$$\alpha<\alpha_{th}=1.303(\varepsilon/m)^{4/3}(\beta_c/\omega_0)^{2/3}.$$

Finally, we present a more physical argument [7,16] for estimating the threshold for autoresonance in the system. Assume a continuing phase locking in the system, so that the phase mismatch Φ remains bounded and small, $|\Phi|\ll\pi$, while the amplitude a_1 is a slow function of time. Then Eq. (4b) can be approximated as

$$\Phi_t\approx\tilde{\beta}_c a_1^2-\alpha t-\frac{\tilde{\varepsilon}}{2a_1}, \tag{7}$$

which, upon differentiation and use of Eq. (4a), yields

$$\Phi_{tt}\approx-S\sin\Phi-\alpha, \tag{8}$$

where $\tilde{\varepsilon}=\varepsilon/m\omega_0$, $\tilde{\beta}_c=\omega_0\beta_c$, and $S(t)=\tilde{\varepsilon}[\tilde{\beta}_c a_1+\tilde{\varepsilon}/(4a_1^2)]$ is a slow function of time. Equation (8) represents an effective adiabatic pendulum problem for the variable Φ. It shows that in the phase-locked state, Φ oscillates around some average, provided the effective tilted cosine potential

$$V_{\rm eff}=\alpha\Phi-S\cos\Phi \tag{9}$$

governing the dynamics of Φ has potential minima. The condition for existence of minima is $S>\alpha$. On the other hand, the function S as a function of a_1 has a minimum $S_m=3/2\tilde{\varepsilon}^{4/3}\tilde{\beta}_c^{2/3}$ at $a_{1m}=1/2(\tilde{\varepsilon}/\tilde{\beta}_c)^{1/3}$. Then the requirement for having effective potential minima at all stages of evolution, i.e., $S_m>\alpha$, yields $\tilde{\varepsilon}>(2\alpha/3)^{3/4}\tilde{\beta}_c^{-1/2}=0.738\alpha^{3/4}\tilde{\beta}_c^{-1/2}$. Thus, to within a few percent in the coefficient, we recover the above-mentioned threshold condition (6).

III. QUANTUM-MECHANICAL LADDER CLIMBING

The LC phenomenon is, in some sense, the quantum analog of the classical dynamic AR. The quantum energy levels of the nonlinear oscillator described by Eq. (1) are [17]

$$E_n\approx\hbar\omega_0[(n+1/2)-\beta_q(n+1/2)^2], \tag{10}$$

where $\beta_q=(\hbar/m\omega_0)\beta_c$.

This distribution of levels can be viewed as a ladder in which the distance between adjacent steps decreases as one climbs to higher energy. In order to continue from one step in the ladder to another, one has to adjust the driving frequency so that initially it matches $(E_1-E_0)/\hbar$ and, after the probability of finding the system in level one reaches unity, change the driving frequency to match $(E_2-E_1)/\hbar$, and so on. Equation (10) defines the transition frequency:

$$\omega_{n,n+1}=(E_{n+1}-E_n)/\hbar=\omega_0[1-2\beta_q(n+1)]. \tag{11}$$

Therefore, at every step, one has to change the driving frequency by $2\omega_0\beta_q$, wait a certain time until the probability for transition from level n to level $n+1$ approaches unity (but not more than this time, since otherwise the probability of returning to level n starts to increase), and change the drive frequency again. This is a very different strategy as compared to the classical AR, where the frequency is varied continuously without any feedback information being necessary during the excitation process. The question is how excitation of the quantum nonlinear oscillator proceeds if one *passes* the transition frequencies by continuously varying the driving frequency. Prior to discussing this issue, it is useful to introduce three relevant time scales in our problem, i.e., the Rabi time scale T_R, the sweep rate time scale T_S, and the nonlinear transition time scale T_{NL}, which are defined as follows:

$$T_R=1/\Omega_R=\sqrt{2m\hbar\omega_0}/\varepsilon, \tag{12a}$$

$$T_S = 1/\sqrt{\alpha}, \tag{12b}$$

$$T_{NL} = 2\omega_0\beta_q/\alpha = 2\hbar\beta_c/m\alpha. \tag{12c}$$

From the Landau-Zener theorem we know that efficient population transfer by a chirped pulse in two-level systems can be achieved [18,19] if $\Omega_R^2/2\alpha > 1$. In terms of the above-mentioned time scales this condition can be expressed as

$$T_R < \frac{T_S}{\sqrt{2}}. \tag{13}$$

Note that T_S is the characteristic time for population transfer within the two-level system driven by chirped frequency radiation, while T_{NL} is the time necessary for the chirped frequency to pass the nonlinear shift between two adjacent energy levels. Therefore, the condition

$$T_S < T_{NL} \tag{14}$$

guarantees completion of the population exchange between two adjacent levels before the varying driving frequency passes the resonance with the next transition. Note that Eq. (14) is only a necessary condition for being in the LC regime, where successive resonant transitions between adjacent levels are effectively independent. A stronger, but sufficient, condition must take into account what usually is referred to as the *width* of the resonance. In other words, to have the LC process, the driving amplitude must be sufficiently small, so that only two adjacent levels are coupled at each given time of chirped excitation. We shall discuss this effect and find a stronger inequality to replace (14) for the LC in the following.

IV. TRANSITION FROM LC TO AR

At this stage, we further discuss the LC versus AR regimes and the transition from one regime to another. First, we focus on the condition for classicality in our problem. Application of the classical theory requires mixing (coupling) of many levels at all times. In our case, the driving force amplitude is a parameter that can cause such mixing. In other words, for classicality, the *width* of the resonance should be sufficient to include, in addition to $\omega_{n,n+1}$, the resonance at $\omega_{m,m+1}$, where $(n-m)$ is the number of levels mixed by the driving force. From a detailed analysis by Goggin and Milonni [20], the condition for a simultaneous resonance with the two transitions is

$$\varepsilon\sqrt{\hbar/2m\omega_0} > 2\hbar\omega_0\beta_q(n-m)^2. \tag{15}$$

If we set the transition to the classical behavior at $(n-m)=1$, we can write this condition in terms of our characteristic times T_R, T_S, and T_{NL} as follows:

$$T_S^2/(T_R T_{NL}) > 1. \tag{16a}$$

The inequality (16a) will be the condition for classical behavior of the system. The inverse inequality

$$T_S^2/(T_R T_{NL}) < 1 \tag{16b}$$

means decoupling between the adjacent resonances. Therefore, Eqs. (13) and (16b) comprise a set of inequalities defining the LC regime [note that (16b) is a stronger inequality than (14) and thus replaces the latter at this stage of discussion].

Next, we write the classical condition for being in the AR regime, i.e.,

$$\varepsilon > \varepsilon_{th}, \tag{16c}$$

where the threshold driving amplitude ε_{th} is given by Eq. (6). By using our three characteristic time scales, (16c) becomes

$$T_R^2/(T_S T_{NL}) < 1.48. \tag{16d}$$

Remarkably, the Planck constant present in T_R and T_{NL} cancels in (16d). Thus, conditions (16a) and (16d) define the regime of classical AR.

At this stage, to visualize the different regimes of operation, we introduce two dimensionless parameters $P_1 = T_S/T_R$ and $P_2 = T_{NL}/T_S$. The pair of inequalities (13) and (16b), which guarantee efficient continuing excitation in the LC regime, can be written in terms of these parameters as

$$P_1 > \sqrt{2} \tag{17}$$

and

$$P_2 > P_1. \tag{18}$$

Similarly, the classical autoresonance conditions (16a) and (16d) become

$$P_2 < P_1 \tag{19}$$

and

$$P_2 > 0.67/P_1^2. \tag{20}$$

All these inequalities divide the P_1-P_2 parameter space into a number of regions, as shown in Fig. 1. The region corresponding to the quantum-mechanical LC is separated from the classical AR region by the shaded transition area. We illustrate all these conditions in the next section, by presenting quantum-mechanical simulations for two sets of conditions, as one crosses the boundary with either the LC or the AR regime.

Finally, we expect that the usual energy relaxation processes in molecular systems will not affect the efficiency of excitation in either the AR on LC regime, provided the duration of the excitation process is short compared to the characteristic relaxation time scale.

V. NUMERICAL SIMULATION

Here we present the results of numerical simulations which test the above-mentioned predictions. We solved the normalized time dependent Schrödinger equation for a particle in the Morse potential $U(\xi) = (D/\hbar\omega_0)[1-\exp$

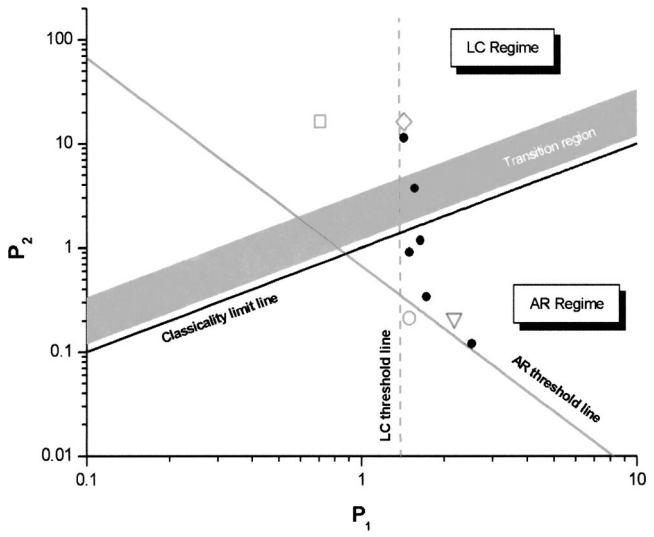

FIG. 1. P_1-P_2 parameter space. The full circles correspond to thresholds found in numerical simulations. Open triangle, square, diamond, and circle are points at which detailed simulation results are shown in Figs. 3–6 below. The gray area is the transition between the quantum-mechanical and classical regimes. Note that the linear oscillator limit requires $P_2 \to 0$ and therefore cannot be in neither LC nor AR regime.

$(-a\xi)]^2$ (see the illustration in Fig. 2) perturbed by a spatially uniform, oscillating, chirped frequency driving force, so that the perturbing Hamiltonian is $H' = (\varepsilon x_0/\hbar\omega_0)\xi \sin(t - 0.5\alpha t^2)$, where $x_0 = \sqrt{\hbar/m\omega_0}$.

We used the well-known Morse functions ψ_n of the unperturbed oscillator to calculate the dipole matrix elements $H_{m,n} = \langle \psi_n | \xi | \psi_m \rangle$ and used this matrix in solving the vector equation [17]

$$i\dot{C}_m = \sum_n H_{m,n} C_n , \tag{21}$$

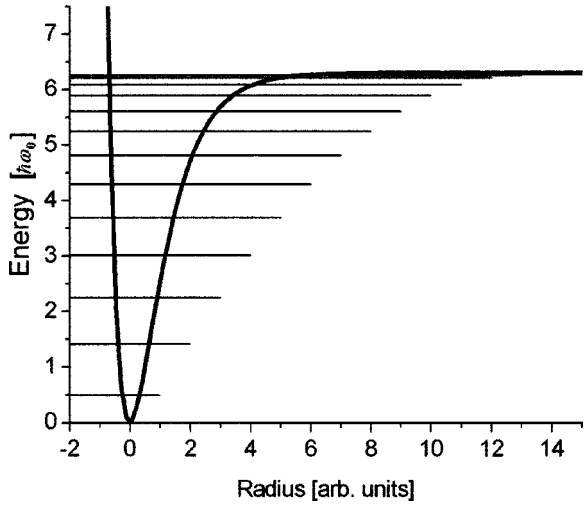

FIG. 2. The Morse potential and its energy levels. One can see that the distance between adjacent levels decreases as one climbs into higher energy levels on the ladder. Parameters are $D = 6.3\hbar\omega_0$ and $a = 1$.

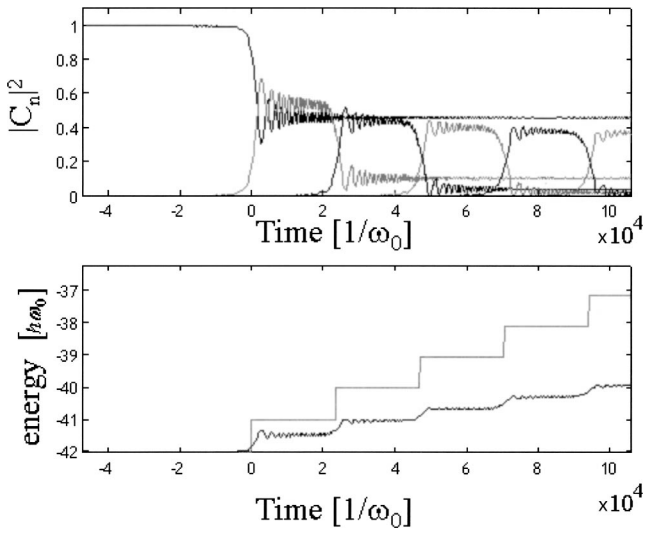

FIG. 3. The results of numerical simulation with $(P_1, P_2) = (0.71, 16.3)$ (open square in Fig. 1). P_1 is below the threshold for efficient LC. The upper graph shows the probabilities of different levels as a function of time. The lower graph presents the energy of the oscillator as a function of time, as well as the maximum possible energy one could reach in the case of complete transfer of population between the levels.

where C_n are the complex amplitudes in the expansion $\psi(t) = \Sigma_n C_n(t)\psi_n$. We used the initial conditions $C_0 = 1$ and $C_n = 0$, $n > 0$, corresponding to the oscillator at rest. No attempt was made to deal with the continuum of states associated with the dissociation. Figures 3–6 show the results of our simulation at four different points in the P_1-P_2 plane (see Fig. 1).

Figures 3 and 4 illustrate the quantum-mechanical regime of operation with well-separated transitions between successive levels. In contrast, Figs. 5 and 6 illustrate strong coupling between many neighboring levels during the excitation process, indicating the classical behavior.

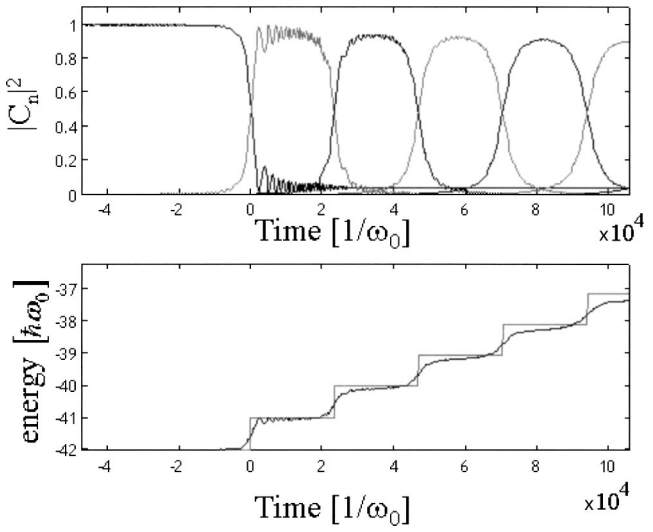

FIG. 4. The same as Fig. 3 but at point $(P_1, P_2) = (1.43, 16.3)$ (open diamond in Fig. 1). P_1 is above the threshold for efficient LC.

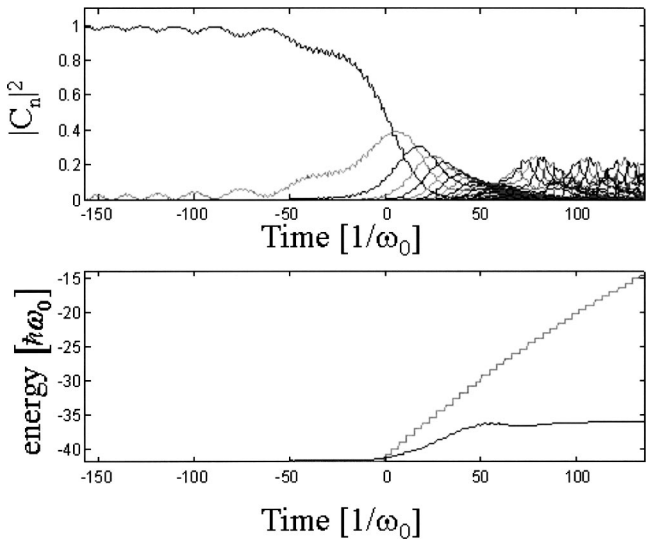

FIG. 5. The same as Fig. 3 but at point $(P_1,P_2)=(1.49,0.21)$ (open circle in Fig. 1). P_1 is below the threshold for classical AR.

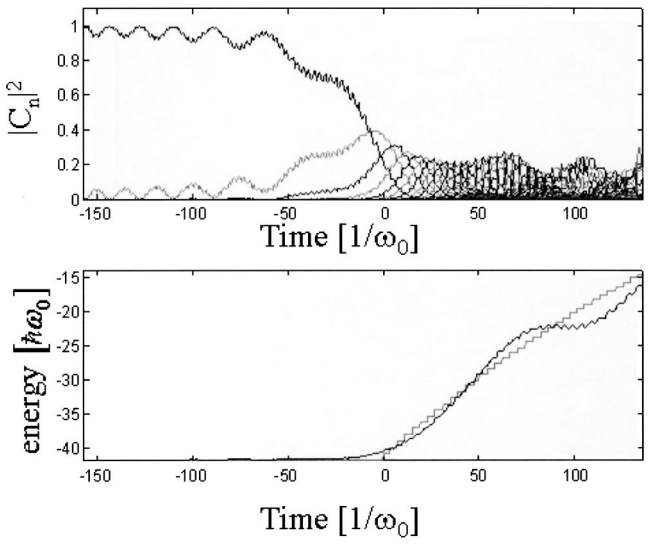

FIG. 6. The same as Fig. 3 but at point $(P_1,P_2)=(2.17,0.21)$ (open triangle in Fig. 1). P_1 is above the threshold for classical AR.

VI. CONCLUSIONS

(a) We have discussed two adiabatic counterparts yielding efficient excitation of oscillating systems from equilibrium by passage through resonance, i.e., quantum-mechanical ladder climbing and classical dynamic autoresonance.

(b) We characterized the process of chirped frequency excitation by three characteristic time scales T_R, T_S, T_{NL}, i.e., the Rabi, sweep, and nonlinearity time scales. These three times can be used to conveniently parametrize the excitation process in a dimensionless two-parameter space $P_1=T_S/T_R$ and $P_2=T_{NL}/T_S$.

(c) Conditions for the transition between the quantum-mechanical and classical behavior in the process of adiabatic, chirped frequency excitation were found.

(d) If the condition for classicality is met, a more transparent classical theory can be used instead of the quantum-mechanical formalism. This yields significant simplification and insight in analyzing the driven system.

(e) Finally, two main conditions define the region in P_1-P_2 parameter space for efficient, chirped frequency excitation in either the LC or AR regime, i.e.,

$$P_1>\sqrt{2} \quad \text{and} \quad P_1>\frac{1}{0.82\sqrt{P_2}}.$$

ACKNOWLEDGMENT

This work was supported by the Israel Science Foundation under Grant No. 187/02.

[1] A. Ben-Shaul, Y. Haas, K. L. Kompa, and R. D. Levine, *Laser and Chemical Change* (Springer-Verlag, Berlin, 1981).
[2] D. J. Maas, D. I. Duncan, B. R. Vrijen, W. J. van der Zande, and D. L. Noordam, Chem. Phys. Lett. **290**, 75 (1998).
[3] S. Chelkowski, A. D. Bandrauk, and P. B. Corkum, Phys. Rev. Lett. **65**, 2355 (1990).
[4] B. Meerson and L. Friedland, Phys. Rev. A **41**, 5233 (1990).
[5] J. M. Yuan and Wing-Ki Liu, Phys. Rev. A **57**, 1992 (1998).
[6] T. Witte, T. Hornung, L. Windhorn, D. Proch, R. de Vivie-Riedle, M. Motskus, and K. L. Kompa, J. Chem. Phys. **118**, 2021 (2003).
[7] M. S. Livingston, *High-Energy Particle Accelerators* (Interscience, New York, 1954).
[8] L. Friedland, Phys. Rev. E **59**, 4106 (1999).
[9] J. Fajans, E. Gilson, and L. Friedland, Phys. Rev. Lett. **82**, 4444 (1999).
[10] J. Fajans, E. Gilson, and L. Friedland, Phys. Plasmas **6**, 4497 (1999).
[11] I. Aranson, B. Meerson, and T. Tajima, Phys. Rev. A **45**, 7500 (1992).
[12] L. Friedland and A. G. Shagalov, Phys. Rev. Lett. **81**, 4357 (1998).
[13] R. Malhotra, Sci. Am. **281**(5), 56 (1999).
[14] L. Friedland, Astrophys. J. **547**, L75 (2001).
[15] L. D. Landau and E. M. Lifshitz, *Mechanics*, 3rd ed. (Pergamon, Oxford, 1976), Vol. 1, Chap. V, p. 87.
[16] L. Friedland and J. Fajans, Am. J. Phys. **69**, 1096 (2001).
[17] L. D. Landau and E. M. Lifshitz, *Quantum Mechanics (Non-Relativistic Theory)*, 3rd ed. (Butterworth Heinemann, Oxford, 1977), Vol. 3, Chap. VI, p. 136.
[18] S. Chelkowski and A. D. Bandrauk, J. Chem. Phys. **99**, 4279 (1993).
[19] J. R. Rubbmark, M. M. Kash, M. G. Littman, and D. Kleppner, Phys. Rev. A **23**, 3107 (1981).
[20] M. E. Goggin and P. W. Milonni, Phys. Rev. A **37**, 796 (1988).